Accepted Manuscript

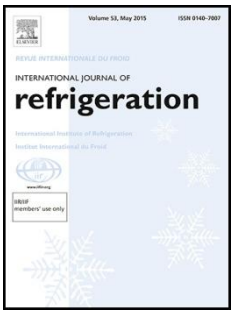

Title: Theoretical and experimental investigation of a combined r134a and transcritical CO_2 heat pump for space heating

Author: Dongfang Yang, Yulong Song, Feng Cao, Lei Jin, Xiaolin Wang

PII: S0140-7007(16)30227-4
DOI: http://dx.doi.org/doi: 10.1016/j.ijrefrig.2016.07.016
Reference: JIJR 3389

To appear in: *International Journal of Refrigeration*

Received date: 1-1-2016
Revised date: 18-7-2016
Accepted date: 24-7-2016

Please cite this article as: Dongfang Yang, Yulong Song, Feng Cao, Lei Jin, Xiaolin Wang, Theoretical and experimental investigation of a combined r134a and transcritical CO_2 heat pump for space heating, *International Journal of Refrigeration* (2016), http://dx.doi.org/doi: 10.1016/j.ijrefrig.2016.07.016.

Theoretical and Experimental Investigation of a Combined R134a and Transcritical CO_2 Heat Pump for Space Heating

Dongfang Yang [a], Yulong Song [a], Feng Cao [a*], Lei Jin [a], Xiaolin Wang [b]

[a] School of Energy and Power Engineering, Xi'an Jiaotong University, Xi'an710049, China

[b] School of Engineering and ICT, University of Tasmania, Private bag 65, Hobart, TAS 7001, Australia

[*]Corresponding author, Email: fcao@mail.xjtu.edu.cn; Tel: 86-29-82663583; Fax: 86-29-82663583

Highlights

- A novel combined R134a and Transcritical CO_2 heat pump was studied.
- Ambient temperature had a large effect on the system performance.
- The system offered a stable temperature hot water with a better performance.
- The comparison results showed that the system improved the COP by up to 22%.

Abstract

In this paper, a novel combined R134a and transcritical CO_2 system was studied theoretically and experimentally for space heating. Experimental results showed that the ambient and space heating temperatures substantially affected the system performance. At the heating requirement with 50 °C in feed water temperature and 70 °C in supply water temperature, the heating capacity and Coefficient of Performance (COP) increased by 32.6% and 18.2%, respectively as the ambient temperature increased from -20 °C to 0 °C. The system COP increased by up to 15% at fixed ambient condition as the feed and supply water temperature decreased from 50 °C/70 °C to 40 °C/50 °C. A mathematical model was also developed and validated using experimental data. The model was used to investigate the performance improvement of the combined system in comparison to the standard transcritical CO_2 system. The comparison results showed that the combined system improved the COP by up to 22%.

Keywords: Transcritical CO_2 heat pump, space heating, COP, heating capacity

Nomenclature

A	Heat transfer area (m^2)	Subscripts	
c_p	Specific heat capacity ($kJ \cdot kg^{-1} \cdot K^{-1}$)	av	Average
d	moisture content (g/kg)	air	air
D	Diameter (m)	cond	Condenser
f	Friction factor	comp	Compressor
h	Enthalpy ($kJ \cdot kg^{-1}$)	CO_2	CO_2 cycle
H_{eq}	equivalent height of the hexagon fin	d	Discharge
j	Local discrete element	dew	Dew point
K	Overall heat transfer coefficient ($W \cdot K^{-1} \cdot m^{-2}$)	eq	Equivalent
M	Molecular weight (kg)	eva	Evaporator
$\dot{m}$	Mass flow rate ($kg \cdot s^{-1}$)	f	fin
N	Number of discrete elements in the exchangers	gc	Gas-cooler
Pr	Prandtl number	h	Heating
$\dot{Q}$	Heat transfer rate (kW)	i	Inner
R	Fouling resistance ($K \cdot m^2 \cdot W^{-1}$)	in	System inlet
Re	Reynolds number	is	Isentropic
T	Temperature (℃)	j	Number of the micro-unit
$\dot{W}$	Power consumption (kW)	out	System outlet
α	Convective heat transfer coefficient ($W \cdot K^{-1} \cdot m^{-2}$)	o	Outer
δ	Thickness of the fin (m)	r	Refrigerant
γ	heat leakage coefficient	s	Suction
η	Efficiency	sg	Single-phase
λ	Conductivity ($W \cdot K^{-1} \cdot m^{-2}$)	tube	tube
ρ	Density ($kg \cdot m^{-3}$)	v	Volumetric
ξ	Dehumidification coefficient	w	Water
		wall	Tube wall
		134a	R134a cycle

1. Introduction

Due to environmental impacts such as ozone depletion and global warming, natural refrigerants such as carbon dioxide (CO_2), water and air have been attracting increasing attention to replace chlorofluorocarbon (CFC) and hydro-chlorofluorocarbon (HCFC) refrigerants in the application areas of refrigeration, heat pump and air-conditioning. Among natural refrigerants, CO_2 has unique characteristics and almost fulfills all required properties to be used as a refrigerant. It has zero ozone depletion potential, very low direct global warming potential, low cost, easy availability, non-flammability, non-toxicity, compatibility with various common materials and compactness due to high operating pressures [Lorentzen, 1990].

Lorentzen [1994] and Riffat et al. [1997] through their pioneering studies proved that the use of CO_2 as a refrigerant can provide an efficient and environmentally attractive technology for air-conditioning, hot water heating and steam production, by operating the system in the transcritical region. Wang et al. [2013] demonstrated that the air-source CO_2 transcritical heat pump could be used as an effective water heater due to its large temperature glide in the gas cooler. However, the transcritical CO_2 refrigeration system has a lower COP due to its high level of irreversibility caused by the superheated vapor horn and the high throttling losses. Hence researchers have put a lot of effort into improving the efficiency of transcritical CO_2 systems by using various cycle modifications employing internal heat exchanger (IHX), expanders, ejectors and subcooling techniques.

Some researchers experimentally studied the performance of the use of the IHX technology in single-stage transcritical CO_2 refrigeration systems [Aprea C. et al.,

2008; Sánchez D. et al., 2010; Torrella E et al., 2011] while others investigated the improvement of the use of IHX in two-stage systems [Cavallini A. et al., 2005; Cavallini A. et al., 2007]. Aprea et al. [2008] experimentally evaluated the energy performance of the transcritical CO_2 system using an IHX. Results showed that the cycle COP was improved by up to 10.5% with use of IHX as the air temperature at gas-cooler inlet decreased from 40 to 25 °C. Torrella et al. [2011] experimentally investigated the performance of an IHX operating in a CO_2 transcritical refrigeration plant at three evaporating levels (-5 °C, -10 °C and -15 °C) and two different gas-cooler outlet temperatures (31 °C and 34 °C). The results showed a maximum increment on cooling capacity of 12% and an increment of the cycle efficiency up to 12%. Cavallini et al. [2005, 2007] experimentally and theoretically studied the performance of a two-stage compression cycle with an IHX. The experimental analysis indicated that IHX increased the specific cooling capacity and reduced the optimum high pressure. Hence the use of the IHX could improve the cycle COP up to approximately 10%. Cho et al. [2009] further experimentally investigated the effect of vapor extraction from the vessel and subsequent injection into the refrigeration cycle in a double-stage system. The system COP improved by 16.5%. Cabello et al. [2012] experimentally analyzed the effect of vapor injection in a single-stage machine and found improvements in system COP up to 7%. Sarkar and Agrawal [2010] investigated the improvement using a parallel compression economization in a transcrictical CO_2 system and observed a maximum improvement of 47.3% in optimum COP during the studied range.

Subcooling technology is another approach to improving the performance of transcritical CO_2 systems. Sarkar [2013] theoretically studied the performance of a transcritical CO_2 system using a thermoelectric device to subcool the refrigerant at the

exit of the gas-cooler. The theoretical results showed that the COP improvement could be up to 25.6%. Llopis R. et al. [2015] further studied energy improvements of CO_2 refrigeration cycles using dedicated mechanical subcooling. The improvement in COP and cooling capacity was up to 20% and 28.8%, respectively.

Recently, performance improvements in transcritical CO_2 systems were also considered by combining them with other thermal systems via heat recovery in the gas-cooler [Arora et al., 2011; Aprea et al., 2015]. Arora et al. [2011] theoretically studied a transcritical CO_2 system combined with a BrLi-H_2O absorption system. Aprea et al. [2015] analyzed the combination of the transcritical CO_2 system with a desiccant wheel for air-conditioning purposes.

The above-mentioned technologies have demonstrated the potential to improve performance of transcritical CO_2 systems. However, these technologies have their own application limits. For instance, IHX technology may cause substantial superheating at the compressor inlet. Sub-cooling technology still lacks experimental studies to support the theoretical findings. Furthermore, these technologies have not been tested under the conditions required for building space heating due to high feed water temperatures (40 – 50 °C). In this study, a combined R134a and transcritical CO_2 heat pump is proposed. The R134a refrigeration system is used not only to produce the hot water, but also to subcool the feed water before it enters the gas-cooler of the transcritical CO_2 system. The performance of the combined system is experimentally studied and a mathematical model is also developed to investigate the improvement of the combined system in comparison to the standard transcritical CO_2 system.

2. System description

Fig.1 shows a schematic drawing of the combined system which includes an R134a subsystem, a transcritical CO_2 subsystem, a three-way valve, a mixing tank, and a circulating water pump. The ambient temperature is controlled from -20 to 10 °C. The warm feed water (return water from space heating user in this study) at a temperature of 40 to 50 °C flows through the three-way valve and then is split into two streams. The first stream of feed water flows into the condenser of the R134a cycle where it is heated up by the high temperature R134a refrigerant. Thereafter this stream of hot water is channeled into the mixing tank. Another stream of feed water flows into the evaporator of the R134a cycle where it is cooled down by the R134a refrigerant. Cold water from the R134a cycle evaporator is then channeled into the gas-cooler of the transcritical CO_2 cycle where the cold water subcools the CO_2 and hence is heated up by the high temperature CO_2. This stream of hot water is introduced into the mixing tank where it is mixed with the first stream of hot water from the R134a cycle. In the system, water is used as an intermediate fluid to link the transcritical CO_2 cycle and R134a cycle.

Fig. 2 shows a pressure-enthalpy (P-h) diagram of the two cycles in the combined system. It shows that the evaporation temperature in the R134a cycle increases from ambient temperature up to around 15 °C which is much higher than the ambient temperature in winter. This guarantees the performance of the R134a cycle. In the transcritical CO_2 cycle, CO_2 at the gas cooler outlet is sub-cooled from point 5 to point 3 by cold water from the evaporator of the R134a cycle. It is well-known that subcooling CO_2 in the gas-cooler improves the system COP. Hence the transcritical CO_2 cycle has potential to offer a better system COP via subcooling.

3. Experimental setup and error analysis

3.1 Experimental setup

Fig. 3 is a picture of the experimental prototype combined R134a and transcritical CO_2 system. The experiment is performed in an environmental laboratory, which consists of an environmental chamber to control the ambient temperature and humidity, and a water supply system to control the feed water temperature and volume flow rate. The dry-bulb temperature of the environmental chamber is controlled in a range from -20 to 10 °C. The feed water temperature is controlled between 40 and 50 °C. The three-way proportional valve is used to adjust the water flow ratio between the R134a and CO_2 cycles. A Bitzer semi-hermetic reciprocating compressor (12 $m^3 \cdot h^{-1}$ in displacement) is used in the transcritical CO_2 cycle with a given isentropic efficiency $\eta_{s,co} = 0.65$ at test conditions, and a Copeland scroll compressor (35 $m^3 \cdot h^{-1}$ in displacement) is employed in the R134a cycle with a given $\eta_{s,134} = 0.75$ at test conditions. The details of the system components are listed in Table 1.

The experimental prototype is well instrumented and the measurement points are indicated in Fig. 1. The compressor power consumption is measured by an electric power meter (QINGZHI, 8901F) with an accuracy of ±0.25% of reading for the CO_2 compressor, and an electric power analyzer (YOKOGAWA, WT-500) with an accuracy of ±0.1% of full scale (0 - 120 kW) for the R134a compressor, respectively. The temperatures are measured by Class-A type RTD sensors (PT100) with an accuracy of ±0.2 °C for water, and sheathed type K thermocouples with an accuracy of ±0.5 °C for refrigerant, respectively. Refrigerant pressures are measured by pressure transmitters (±0.25% of full scale) with a measuring range of 0 – 6 MPa for the R134a cycle and the low pressure side of the CO_2 cycle, and 0 – 16 MPa for the high pressure side of CO_2 cycle, respectively. The water volume flow rates are measured by a turbine flow meter (±0.5% of full scale) with a measuring range of 0~6000 $L \cdot hr^{-1}$. All the measurement data including electrical power, temperature,

pressure, and volume flow rate are collected by a calibrated data acquisition system (HP34970A of Agilent). The measured data during the experimental process are collected and recorded at a time interval of 10 s.

3.2 Data reduction and error analysis

The measured data is used to evaluate the performance of the combined system. The heating capacity of the combined system is calculated by the water flow rate, $\dot{m}_w$ and the temperature difference between the system inlet (before the three way valve) and outlet (after the mixing tank) of the combined system. It is expressed by:

$$\dot{Q}_h = \dot{m}_w c_p \left(T_{w,out} - T_{w,in}\right) \tag{1}$$

where c_p is the specific heat of the water at constant pressure. $T_{w,in}$ and $T_{w,out}$ represent the hot water temperature at the system inlet and outlet, respectively.

The system COP is obtained based on the above calculated heating capacity and the measured total power consumption ($\dot{W}_{comp}$) and can be calculated by:

$$COP = \frac{\dot{Q}_h}{\dot{W}_{comp}} \tag{2}$$

$$\dot{W}_{comp} = \dot{W}_{c,134a} + \dot{W}_{c,CO_2} \tag{3}$$

where $\dot{W}_{134a}$ and $\dot{W}_{CO_2}$ are the compressor power consumption in the R134a and CO_2 cycles, respectively.

The accuracy of the sensors has been listed in the above section. The error propagation for heating capacity and COP is calculated using the Kline and McClintock method as expressed by

$$w_R = \left[\left(\frac{\partial R}{\partial x_1} w_1\right)^2 + \left(\frac{\partial R}{\partial x_2} w_2\right)^2 + \cdots + \left(\frac{\partial R}{\partial x_n} w_n\right)^2\right]^{1/2} \tag{4}$$

where w_R is the resultant uncertainty, w_1, w_2, …, w_n are the uncertainties of the independent variables. R is a given function of the independent variables x_1, x_2, …, x_n. Using this equation, the maximum uncertainties for the heating capacity and COP are

3.15% and 3.58%, respectively.

4. Mathematical model

In order to evaluate the performance of the combined system and compare its performance with the standard transcritical CO_2 system and modified CO_2 cycles, a simple mathematical model is developed based on energy balance. The cycle state points are indicated in Fig. 2.

4.1 Compressor model

Compressor operation is defined in terms of an isentropic efficiency (η_{is}), the mass flow rate ($\dot{m}_r$) and power input ($\dot{W}_c$) of the compressor can be calculated by:

$$\dot{m}_r = \eta_v V_{com,s} \rho_s \tag{5}$$

$$\dot{W}_c = \frac{\dot{W}_{c,is}}{\eta_{is}} = \dot{m}_r \frac{h_{d,is} - h_s}{\eta_{is}} \tag{6}$$

where η_v is the volumetric efficiency which can be calculated by using the Copeland & BITZER compressor type-selection software [Emerson Product Selection Software 1.0.51 for R134a compressors, and BitzerWin 6.4.1 for CO_2 compressors], $\dot{W}_{c,is}$ is isentropic power consumption of the compressor. This model is applicable for the compressors in both the R134a and CO_2 cycles. According to the first law of thermodynamics, work input to the compressors can also be calculated by:

For the compressor in R134a cycle: $\dot{W}_{c,134a} = \dot{m}_{r,134a}\left(h_{d,134} - h_{s,134}\right)$ (7)

For the compressor in CO_2 cycle: $\dot{W}_{c,CO_2} = \dot{m}_{r,CO_2}\left(h_{d,CO_2} - h_{s,CO_2}\right)$ (8)

4.2 Gas cooler model in the CO_2 cycle

Heat transfer in the gas cooler (tube-in-tube heat exchanger) can be calculated according to energy balance. The energy balance equations are:

$$\dot{Q}_{gc} = \dot{m}_{r,CO_2}\left(h_{CO_2,gc-in} - h_{CO_2,gc-out}\right) = \dot{m}_{w,gc} c_p \left(T_{w,gc-out} - T_{w,gc-in}\right) \tag{9}$$

$$\dot{Q}_{gc} = \sum_{j=1}^{N} K_j A_{i,j} (T_{CO_2,j} - T_{w,j}) \tag{10}$$

$$K_j = \left(\frac{1}{\alpha_{CO_2,j}} + \frac{A_{i,j}}{\alpha_{w,j} A_o} + R_{w,j} \right)^{-1} \tag{11}$$

where $\alpha_{CO_2,j}$ is the local heat transfer coefficient of CO_2 which can be calculated using the correlations for supercritical CO_2 proposed by Dang and Hihara [2004]. $\alpha_{w,j}$ is the heat transfer coefficient of water which can be calculated using the Dittus-Boelter correlation.

4.3 Evaporator model in the CO_2 cycle

The evaporator in the CO_2 system is a finned tube heat exchanger which is typically a cross-flow heat exchanger. For CO_2 and air side, energy balance and heat transfer rate equations can be expressed by:

$$\dot{Q}_{eva} = \dot{m}_{r,CO_2} \left(h_{CO_2,eva-out} - h_{CO_2,eva-in} \right) = \dot{m}_{air} \left(h_{air,out} - h_{air,in} \right) \tag{12}$$

$$\dot{Q}_{eva} = \sum_{j=1}^{N} K_j A_{i,j} (T_{CO_2,j} - T_{air,j}) \tag{13}$$

$$K_j = \left(\frac{1}{\alpha_{CO_2,j}} + \frac{\gamma A_{i,j}}{\alpha_{air,j} \xi \eta_{o,j} A_{o,j}} \right)^{-1} \tag{14}$$

$$\xi = \begin{cases} 1 + 2460 \dfrac{d_{av} - d_{T_{wall}}}{T_{av} - T_{wall}} & T_{wall} < T_{dew} \\ 1 & T_{wall} > T_{dew} \end{cases} \tag{15}$$

$$h_{av} = h_{T_{wall}} + \frac{h_{in} - h_{out}}{\ln \left(\dfrac{h_{in} - h_{T_{wall}}}{h_{out} - h_{T_{wall}}} \right)} \tag{16}$$

$$d_{av} = d_{T_{wall}} + \frac{h_{av} - h_{T_{wall}}}{h_{in} - h_{T_{wall}}} (d_{in} - d_{T_{wall}}) \tag{17}$$

$$h_{T_{wall}} = h(T_w, d_{T_{wall}}) \tag{18}$$

$$T_{av} = T(h_{av}, d_{av}) \tag{19}$$

$$\eta_f = \frac{\tanh(mH_{eq})}{mH_{eq}} \tag{20}$$

$$\eta_o = \frac{1}{A_o} (A_{o,tube} + A_{o,f} \cdot \eta_f) \tag{21}$$

$$m = \sqrt{\frac{2\alpha_{air}}{\lambda_f \delta_f}} \tag{22}$$

where K_j is the overall heat transfer coefficient [Bergman, T. et al. 2011]. The heat transfer coefficient $\alpha_{CO_2,j}$ inside the tube of the evaporator is calculated using the correlation proposed by Cheng et al. [2006]. The fin side heat transfer coefficient $\alpha_{air,j}$ can be calculated using the correlations proposed by Churchill and Bernstein [1977].

4.4 Condenser model in the R134a cycle

Heat transfer in the condenser (tube-in-tube heat exchanger) of the R134a cycle can be calculated according to the following energy balance equations:

$$\dot{Q}_{cond} = \dot{m}_{w,cond} c_p \left(T_{w,cond-out,} - T_{w,cond-in}\right) = \dot{m}_{r,134a} \left(h_{134a,cond-in} - h_{134a,cond-out}\right) \tag{23}$$

$$\dot{Q}_{cond} = \sum_{j=1}^{N} K_j A_{i,j} (T_{134a,j} - T_{w,j}) \tag{24}$$

$$K_j = \left(\frac{1}{\alpha_{134a,j}} + \frac{A_{i,j}}{\alpha_{w,j} A_{o,j}} + R_{w,j} \right)^{-1} \tag{25}$$

where the heat transfer coefficient $\alpha_{134a,j}$ is calculated using correlations proposed by Shah [1979]. $\alpha_{w,j}$ is the heat transfer coefficient of water which can be calculated using the Dittus-Boelter correlation.

4.5 Evaporator model in the R134a cycle

The energy balance in the evaporator (tube-in-tube heat exchanger) of the R134a system can be expressed by

$$\dot{Q}_{eva} = \dot{m}_{w,eva} c_p \left(T_{w,eva-in,} - T_{w,eva-out}\right) = \dot{m}_{r,134a} \left(h_{134a,evap-out} - h_{134a,evap-in}\right) \tag{26}$$

$$\dot{Q}_{eva} = \sum_{j=1}^{N} K_j A_{i,j} (T_{134a,j} - T_{w,j}) \tag{27}$$

$$K_j = \left(\frac{1}{\alpha_{134a,j}} + \frac{A_{i,j}}{\alpha_{w,j} A_{o,j}} + R_{w,j} \right)^{-1} \quad (28)$$

where the heat transfer coefficient $\alpha_{134a,j}$ is calculated using correlations proposed by Kandlikar [1990]. $\alpha_{w,j}$ is the heat transfer coefficient of water which can be calculated using the Dittus-Boelter correlation.

4.6 Performance parameters

For the standard transcritical CO_2 system, the heating capacity and COP are calculated by:

$$\dot{Q}_h = \dot{m}_{r,CO_2} (h_2 - h_3) \quad (29)$$

$$COP = \frac{\dot{Q}_h}{\dot{W}_{c,CO_2}} \quad (30)$$

For the combined system, the heating capacity and COP are calculated by

$$\dot{Q}_h = \dot{m}_{r,CO_2} (h_2 - h_5) + \dot{m}_{r,134a} (h_8 - h_9) \quad (31)$$

$$COP = \frac{\dot{Q}_h}{\dot{W}_{c,CO_2} + \dot{W}_{c,134a}} \quad (32)$$

In the transcritical CO_2 cycle, the cycle COP is affected by the discharge pressure. Wang et al. [2013] proposed a correlation to calculate the optimum discharge pressure as follows:

$$p_{CO_2,d} \cong 23.08391 + 1.22378\ T_{CO_2,w,out} - 0.00407\ T_{CO_2,w,out}^2 + 0.16207\ T_{air}. \quad (33)$$

However, the system mode and operating conditions in the studied system might be different from those reported by Wang et al. (2013). Therefore, the actual optimal discharge pressure could be different from that calculated from the correlation. In the current simulation, this correlation was used to provide a reference discharge pressure at different working conditions. The actual optimum discharge pressure in the transcritical CO_2 cycle was then calculated by adjusting the discharge pressure in a

certain range to reach the maximum COP, which was shown in the flow chart of the CO_2 cycle subroutine in Fig. 4a. In addition, since the CO_2 separator is installed at the evaporator exit to take care of the refrigerant mass variation in the components at different working conditions, the CO_2 at the evaporator exit is always remained at the saturated condition under the studied working conditions. However, as the CO_2 flows from the evaporator exit to the compressor suction, the CO_2 is superheated through heat transfer between the CO_2 and suction pipe, and between CO_2 and motor, etc. In order to consider these heat transfer effects, the superheating of CO_2 at the compressor suction is considered in the model as shown in Fig. 4a.

Figs. 4 and 5 show the simulation flow charts for the combined system and cycle subroutines. The correlations of refrigerant flow rates through expansion valve in different conditions were given from relevant manufacturers. In the simulation, the ambient temperature, ambient air relative humidity, feed hot water temperature, and water volumetric flow rate are given according to the experimental data at a desired working condition. Based on the calculation using Copeland & BITZER type-selection software and the measurement in the tests, the variation of compressor isentropic efficiency was less than 2.5% for both compressors, thus the isentropic efficiency of the compressors was considered constant in order to simplify the simulation. The volumetric efficiency of each compressor was calculated by using Copeland & BITZER type-selection software under each working condition. The pressure and temperature at each component in the whole system is then calculated based on the above models. Enthalpy at each state point is calculated from these pressures and temperatures using the Engineering Equation Solver (Academic Professional V9.206-3D).

5. Results and discussion

The performance of the proposed combined system was experimentally studied under different working conditions. According to China National Standard for space heating, two different heating scenarios are commonly utilized in building space heating: (i) user supply water temperature is 50 °C and feed water (return water) temperature is 40 °C and (ii) user supply water temperature is 70 °C and feed water temperature is 50 °C. The typical ambient temperature ranges from – 20 to 0 °C in winter in China. The relative humidity of the air is fixed at 60%.

5.1 Performance evaluation at different working conditions

The performance evaluation is experimentally investigated for space heating with a feed water temperature of 50 °C and user supply water temperature of 70 °C. Fig. 6 shows the hot water temperature and CO_2 discharge pressure at different ambient temperatures. As the ambient temperature increases from -20 °C to 0 °C, the hot water temperature at the outlet of the CO_2 sub-system, R134a sub-system and combined system remains almost constant. This indicates that the combined system could provide stable hot water output under different ambient conditions. Furthermore, the temperature profiles show that the gas-cooler feed water temperature drops from the normal feed water temperature of 50 °C to a level of temperature of 15 to 20 °C in the transcritical CO_2 cycle. This temperature drop at the gas-cooler inlet substantially subcools the CO_2 refrigerant and hence improves the transcritical CO_2 cycle performance. In the R134a cycle, the evaporation temperature is controlled by the feed hot water temperature which is much higher than the ambient temperature and adjusted by the feed water flow rate. This also indicates that the R134a cycle could have high system efficiency. Therefore, the combination of these two systems benefits each other and hence possesses a potential to improve the performance of the combined system. In addition, an increase in ambient temperature increases the

evaporation temperature in the R134a cycle as indicated by the temperature at the CO_2 cycle inlet. This is mainly caused by an increase in the water flow rate to the gas cooler in the transcritical CO_2 cycle. As the ambient temperature increases, heating capacity of the transcritical CO_2 cycle increases. In order to maintain the hot water temperature at the gas cooler outlet, the water flow rate to the gas cooler has to increase and hence the water flow rate into the R134a evaporator increases, which leads to an increase in the evaporation temperature in the R134a system and hence improves the R134a cycle performance. Meanwhile, the ambient temperature increases the evaporation pressure in the evaporator of the transcritical CO_2 system and hence increases the CO_2 compressor suction pressure in the transcritical CO_2 system.

Fig. 7 shows the performance of the combined system at different ambient temperatures. As the ambient temperature increased from -20 to 0 °C, the total power consumption and heating capacity increased by 15.6% and 32.6%, respectively. As ambient temperature increased, the evaporation pressure went up and hence the refrigeration density at the compressor suction rose. Therefore, the mass flow rate of the refrigerant increased, which increased both the heating capacity and compressor power consumption. The heating capacity was found to increase faster than the total power consumption. This explained the increase in the system COP. As the ambient temperature increased from -20 to 0 °C, the system COP increased by 18.2% which was consistent with the common practice.

Figs. 8 and 9 show hot water temperatures and system performance for space heating with a feed water temperature of 40 °C and a user supply water temperature of 50 °C. The temperature profiles and system performance showed the same trend as those presented for the space heating with the feed water temperature of 50 °C and

user supply water temperature of 70 °C. However, it was found that the system COP increased by up to 15% at the lower temperature space heating requirement.

Table 2 presented the system COP at the different flow ratio which is defined a ratio of the water flow rate to the R134a condenser and the total flow rate to the combined system. The ambient temperature was maintained at -20 °C. At the feed water temperature of 50 °C and supply water temperature of 70 °C, the total water flow rate was 1430 $L \cdot hr^{-1}$. The variation of the system COP was found less than 3% as the flow ratio varied from 73.4% to 78.9%. At the feed water temperature of 40 °C and supply water temperature of 50 °C, the total water flow rate was 1860 $L \cdot hr^{-1}$. The variation of the system COP was found less than 2% as the flow ratio increased from 68.1% to 74.2%. These results indicated that the COP did not show significant change under the experimental flow ratio range at the two space heating conditions if the measurement error was considered. However, since the variation of the flow ratio was small in the experiment, it was hard to clearly justify the effect of flow ratio on the system COP. In addition, optimization of the flow ratio involves many other important parameters such as CO_2 discharge pressure, evaporation temperature in the R134a system, gas-cooler outlet temperature, and feed water temperature and so on. Therefore, future theoretical and experimental work needs to be performed to have better understanding of effect of the flow ratio on the system COP.

5.2 Performance comparison

Fig. 10 showed the comparison between simulated and experimental performance at water feed temperature of 40 °C with supply temperature of 50 °C and water feed temperature of 50 °C with supply temperature of 70 °C, respectively. The ambient temperature varied from -20 to 0 °C. The comparison results showed that the simulation results agreed well with the experimental data. Using standard deviation,

the root mean square (RMS) of the difference between simulated and experimental COP was 4.5%, and between simulated and experimental heating capacity was 3.6%. In addition, low temperature space heating with a feed water temperature of 40 °C and user supply water temperature of 50 °C had lower condensation temperature in the R134a system, in comparison to the high temperature heating condition with the feed water temperature of 50 °C and user supply water temperature of 70℃. This improved the R134a system COP and hence the COP of the combined system as shown in Fig. 10. In addition, Fig. 10 also showed that the heating capacity at the low temperature heating condition was slightly lower than that at the high temperature heating condition. The low feed water temperature lowered the evaporation temperature in the R134a system and hence reduced the evaporation pressure which led to a drop in the R134a density at the compressor suction. Therefore, the R134a mass flow rate decreased and the heating capacity of the R134a cycle dropped slightly at the low temperature heating condition.

Fig. 11 shows the comparsion between the COP for a standard transcritical CO_2 system and the COP of the combined system at water feed temperature of 40 °C with supply temperature of 50 °C and water feed temperature of 50 °C with supply temperature of 70 °C, respectively. At both space heating conditions as specified above, the combined system exhibited much better performance. As the ambient temperature increased from -20 to 0 °C, the improvement of the system COP was up to 22% at the feed water temperature of 50 °C with user supply water temperature of 70 °C, and up to 15% at the feed water temperature of 40 °C with user supply water temperature of 50 °C, respectively. This indicated that the combined system was more effective for high temperature hot water applications. The comparison results also

demonstrated that the combined R134a and transcritical CO_2 system could offer better system performance for space heating under the same operating conditions.

In order to weight the losses introduced by the additional temeprature difference between R134a and water in the R134a evapoarator and between CO_2 and water in the gas-cooler, a performance comparison was performed between the proposed combined system and the semi-cascade system without intermediate fluid [Llopis, R. et al, 2015]. Furthermore, the system performance of the proposed combined system was also compared with those repored in the modified CO_2 cycles in literature such as parallel compression cycle [Sarker and Agrawal, 2010] and ejector cycle [Liu and Groll, 2008; Lawrence, N.D., 2012]. The performance for the mentioned modified systems were calculated using the models proposed in the above corresponding literature, respectively. The main parameters and assumptions such as isentropic efficiencies of nozzles and diffusers, economizer pressure, and heat transfer temperature differences between water and refrigerant, and between refrigerant and air were adapted from the above corresponding literature for the individual system as well. Furthermore, in order to make the fair comparison, the temperature approach is used for the performance simulation for all systems. The comparison was performed under the same operating condition (-10 °C in ambient temeprature, 50 °C in water feed temperature and 70 °C in supply water temperature). The power consumption of the compressor was set around 24 kW for all systems and the individual system was also optimized to reach their optimal performance at the operating condition in the simulation. The assumptions and comparison results were listed in Table 3. It was found that the performance difference between the proposed system and the semi-cascade system without intermediate fluid was negligible. This indicated that the losses caused by the temperature difference due to the intermediate flow was

insignificant. In comparison to the semi-cascade system without intermediate fluid [Llopis, R. et al, 2015], the proposed system with intermediate fluid water is more reliable and convenience since the proposed system was modified from an existing single transcritical CO2 prototype. What's more, the R134a evaporating pressure can be optimized or controlled directly via adjustment of hot water flow rate to the R134a evaporator as the operating condition changes. Furthermore, the COP of the proposed combined system was found to be 23.7% higher than that of the parallel compression system and 30% higher than that of the ejector system. This was mainly because both parallel compression system and ejector cycle were not suitable for applications at high gas-cooler outlet temeprature which was caused by the high feed water temperature. The comparison results indicated that the proposed combined system could offer better performance for space heating.

6. Conclusion

In this study, a prototype combined R134a and transcritical CO_2 heat pump was developed and experimentally studied. The experimental results demonstrated that the combined system could operate reliably and supply stable temperature hot water over a wide range of ambient temperatures and feed water temperatures. The experimental results also showed that ambient temperature had a large effect on the system performance. As the ambient temperature increased from -20 to 0℃, the heating capacity and COP of the combined R134a and transcritical CO_2 heat pump increased by 32.6% and 18.2%, respectively. The lower temperature space heating requirement was found to have better system COP in the experimental study as well. In order to further investigate the improvement of the combined system in comparison to the standard transcritical CO_2 heat pump, a simple mathematical model was developed and validated using experimental data. The comparison results showed that the

combined system could offer higher system COP at experimental ambient and feed water temperatures.

References

[1] Aprea, C., Maiorino, A., 2008. An experimental evaluation of the transcritical CO_2 refrigerator performances using an internal heat exchanger, International Journal of Refrigeration, 31, 1006-1011.

[2] Aprea, C., Greco, A., Maiorino, A., 2015. The application of a desiccant wheel to increase the energetic performances of a transcritical cycle, Energy Convers. Manag. 89, 222-230.

[3] Arora, A., Singh, N.K., Monga, S., Kumar, O., 2011. Energy and exergy analysis of a combined transcritical CO2 compression refrigeration and single effect H2O-LiBr vapor absorption system, Int. J. Exergy 9, 453 – 471.

[4] Bergman, T.L., Lavine, A.S., Incropera, F.P., Dewitt, D.P., 2011. Fundamentals of heat and mass transfer, seventh edition, John Wiley & Sons, Inc. ISBN: 13 978-0470-50197-9.

[5] Cabello, R., Sánchez, D., Patiño, J., Llopis, R., Torrella, E., 2012. Experimental analysis of energy performance of modified single-stage CO_2 transcritical vapor compression cycles based on vapor injection in the suction line, Appl. Therm. Eng., 47, 86 – 94.

[6] Cavallini, A., Cecchinato, L., Corradi, M., Fornasieri, E., Zilio, C., 2005. Two-stage transcritical carbon dioxide cycle optimization: a theoretical and experimental analysis, Int. J. Refrig. 28, 1274-1283.

[7] Cavallini, A., Corradi, M., Fornasieri, E, Zilio, C., 2007. Experimental investigation on the effect of the internal heat exchanger and intercooler effectiveness of the energy performance of a two stage transcritical carbon dioxide cycle, in IIR (Ed.) 22nd International Congress of Refrigeration, Beijin, China, 2007.

[8] Cheng, L., Ribatski, G., Wojtan, L., Thome, J.R., 2006. New flow boiling heat transfer model and flow pattern map for carbon dioxide evaporating inside horizontal tubes, Int. J. Heat and Mass Trans. 49 (21-22), 4082-4094.

[9] Cho, H., Baek, C., Park, C., Kim, Y., 2009. Performance evaluation of a

two-stage CO_2 cycle with gas injection in the cooling mode operation, Int. J. Refrig. 32, 40 - 46.

[10] Churchill, S.W., Bernstein, M., 1977. A correlating equation for forced convection from gases and liquids to a circular cylinder in cross flow, ASME Transactions, Journal of Heat Transfer 99 (2), 300-306.

[11] Dang, C., Eiji, H., 2004. In-tube cooling heat transfer of supercritical carbon dioxide, part 1. Experimental measurement, Int. J. Refrig. 27, 736-747.

[12] Dang, C., Eiji, H., 2004. In-tube cooling heat transfer of supercritical carbon dioxide, part 2. Comparison of numerical calculation with different turbulence models, Int. J. Refrig. 27, 748-760.

[13] Lorentzen, G., Trans-critical vapour compression cycle device: Switzerland, WO 90/07683 [P]. 1990-07-12.

[14] Lorentzen, G., 1994. The use of natural refrigerant: a complete solution to the CFC/HCFC predicament, Int. J. Refrig. 18, 190–197.

[15] Kandlikar, S.G., 1990. A general correlation for saturated two-phase flow boiling heat transfer inside horizontal and vertical tubes, J. Heat Trans. 112, 219-228.

[16] Liu, F., Groll, E.A., 2008. Recovery of throttling losses by a two phase ejector in a vapor compression cycle, International Refrigeration and Air Conditioning Conference, paper 924, PURDUE UNIVERSITY, May 2008.

[17] Llopis, R., Cabello, R., Sánchez, D., Torrella E., 2015. Energy improvements of CO2 transcritical refrigeration cycles using dedicated mechanical subcooling, Int. J. Refrig. 55, 129-141.

[18] Neal D. Lawrence, 2012, Analytical and experimental investigation of two-phase ejector cycles using low-pressure refrigerants. Urbana, Illinois, University of Illinois at Urbana-Champaign, 2012.

[19] Riffat, S.B., Alfonso, C.F., Oliveira, A.C., Reay, D.A., 1997. Natural refrigerants for refrigeration and air-conditioning systems, Appl. Therm. Eng. 17(1), 33–42.

[20] Sánchez, D., Torrella, E., Cabello, R., Llopis, R., 2010. Influence of the superheat associated to a semi-hermetic compressor of a transcritical CO_2 refrigeration plant. Appl. Therm. Eng. 30, 302-309.

[21] Sarkar, J., 2013. Performance optimization of transcritical CO_2 refrigeration cycle with thermoelectric subcooler, Int. J. Energy Res. 37, 121-128.

[22] Sarkar, J., Agrawal, N., 2010. Performance optimization of transcritical CO2

cycle with parallel compression economization, International Journal of Thermal Sciences, 49, 838-843.

[23] Shah, M.M., 1979. A general correlation for heat transfer during film condensation inside pipes, Int. J. Heat and Mass Trans. 22 (4), 547-556.

[24] Torrella, E., Sánchez, D., Llopis, R., Cabello, R., 2011. Energetic evaluation of an internal heat exchanger in a CO2 transcritical refrigeration plant using experimental data, Int. J. Refrig. 34, 40-49.

[25] Wang, S.G., Tuo, H.F., Cao, F., Xing, Z., 2013. Experimental investigation on air-source transcritical CO2 heat pump water heater system at a fixed water inlet temperature. Int. J. of Refrig. 36(3), 701-716.

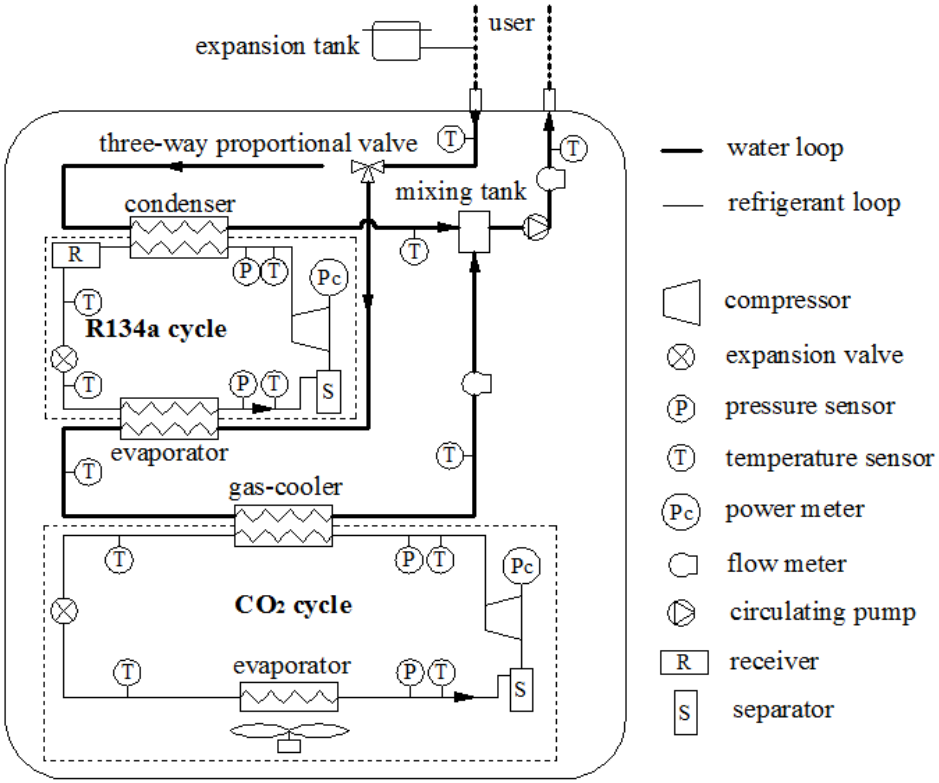

Fig. 1 Schematic drawing of the combined R134a and transcritical CO_2 system

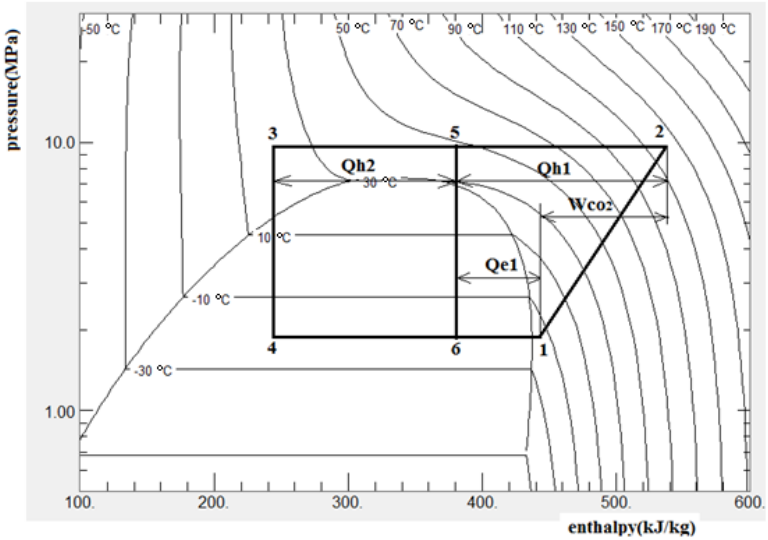

Fig. 2a Pressure-enthalpy (P-h) diagram of the transcritical CO_2cycle

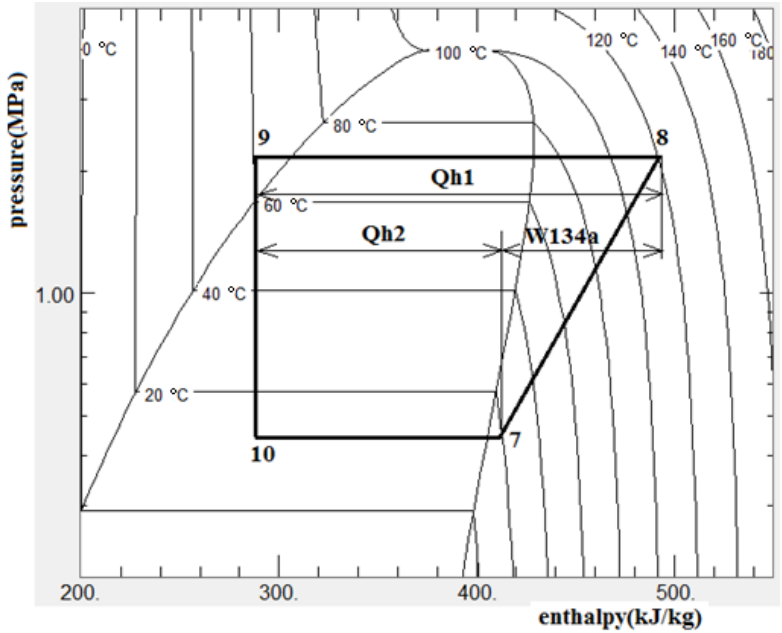

Fig. 2bPressure-enthalpy (P-h) diagram of the R134acycle

Fig. 3A picture of the prototype used in the experiment

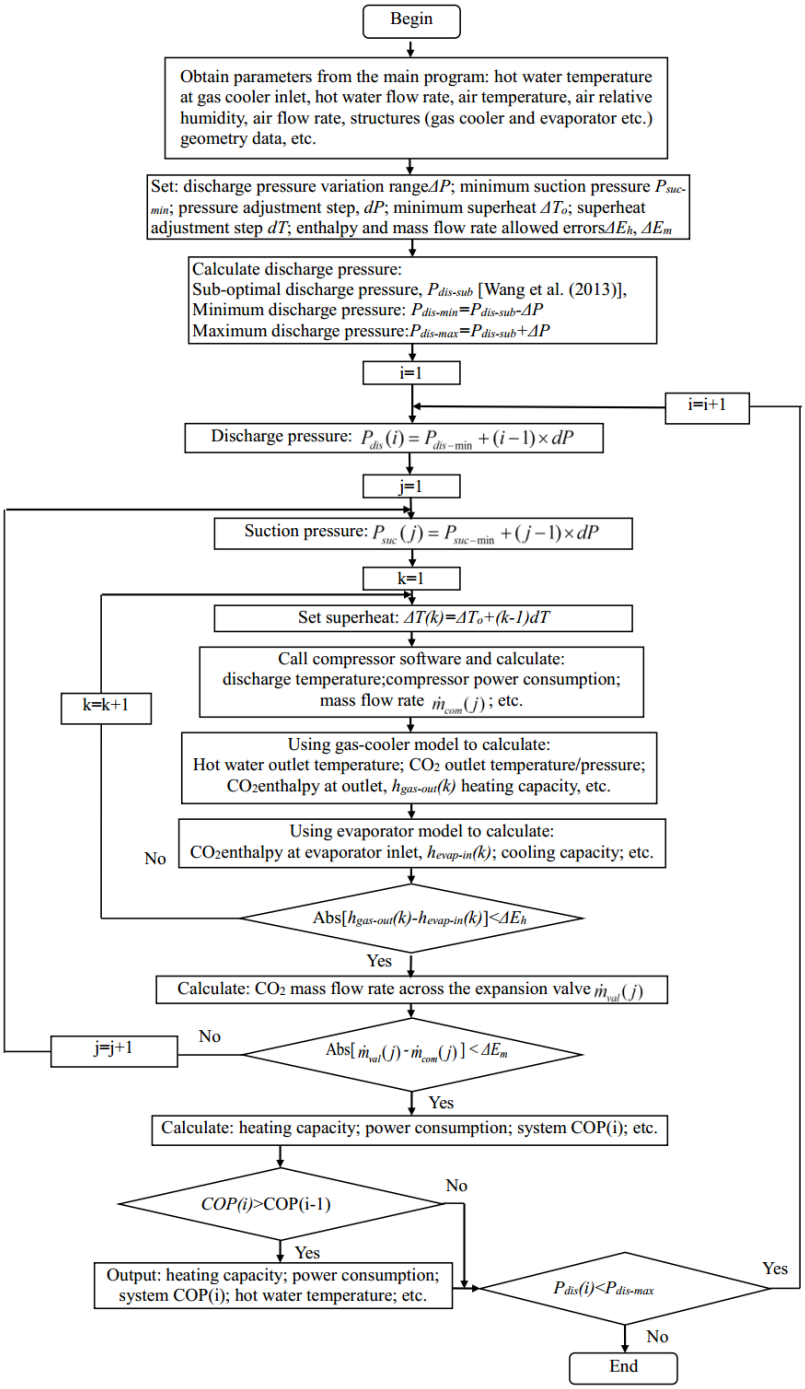

Fig. 4a Flow chart of the transcritical CO2 cycle subroutine

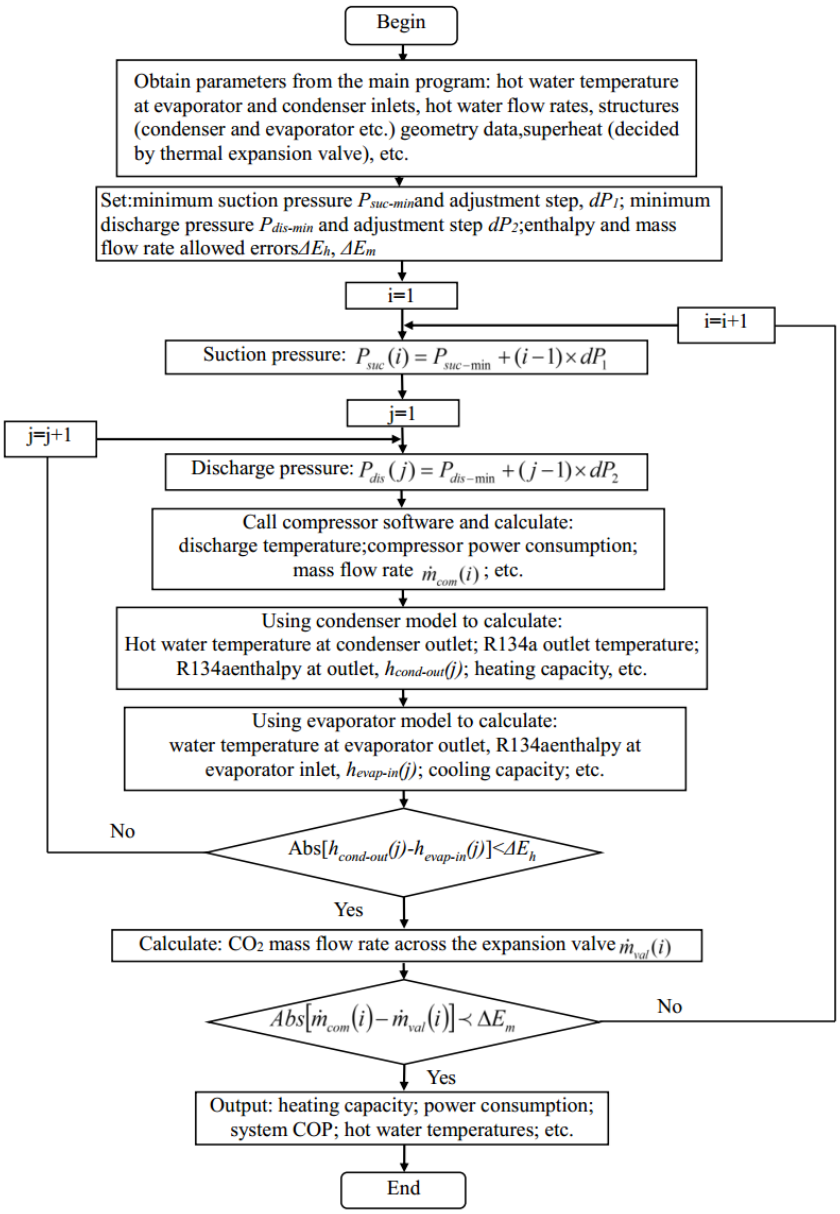

Fig. 4b Flow chart of the R134a cycle subroutine

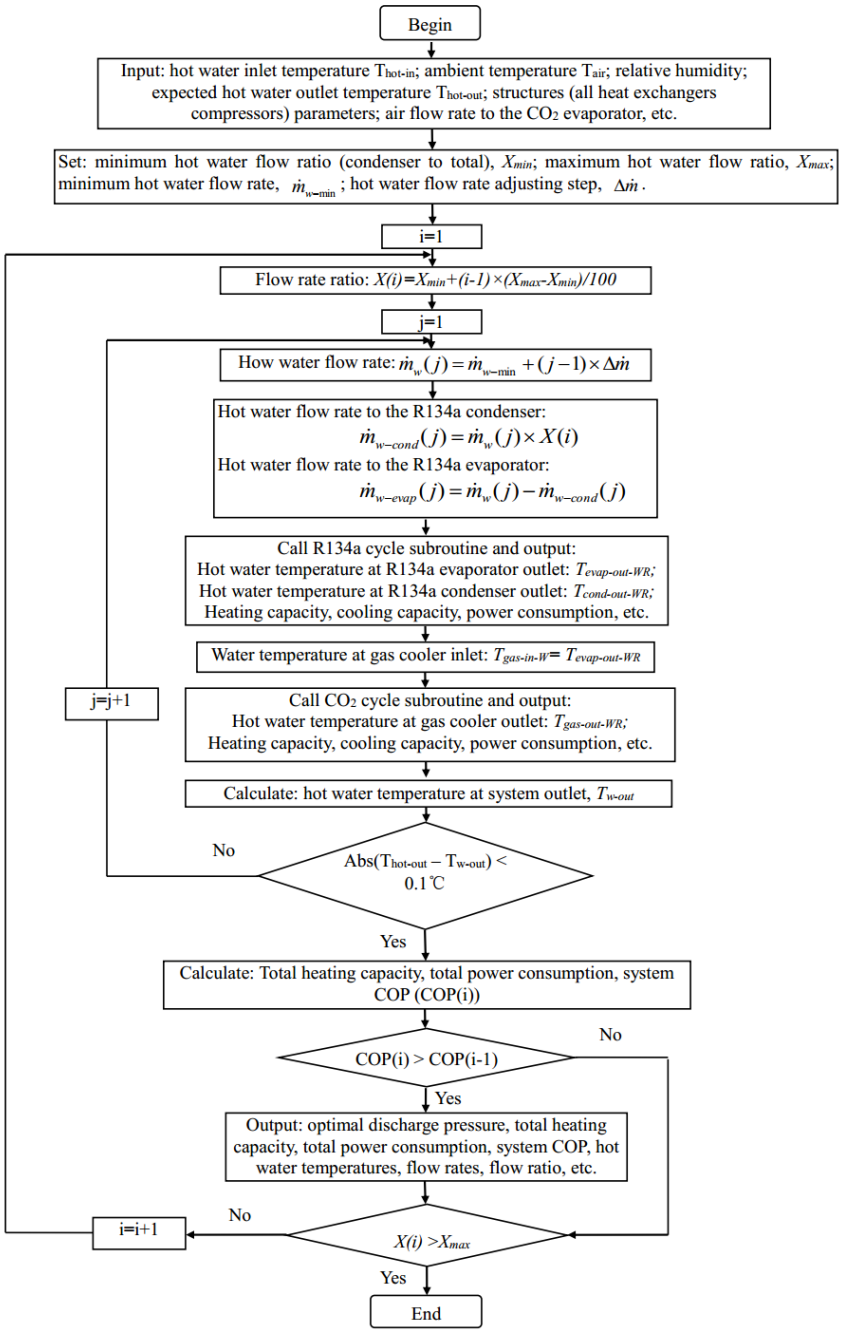

Fig. 5 Simulation flow chart of the proposed combined cycle

Comment [A1]: Author: There are two different Figure 5 captions were provided, and this has been retained. Please check and confirm it is correct.

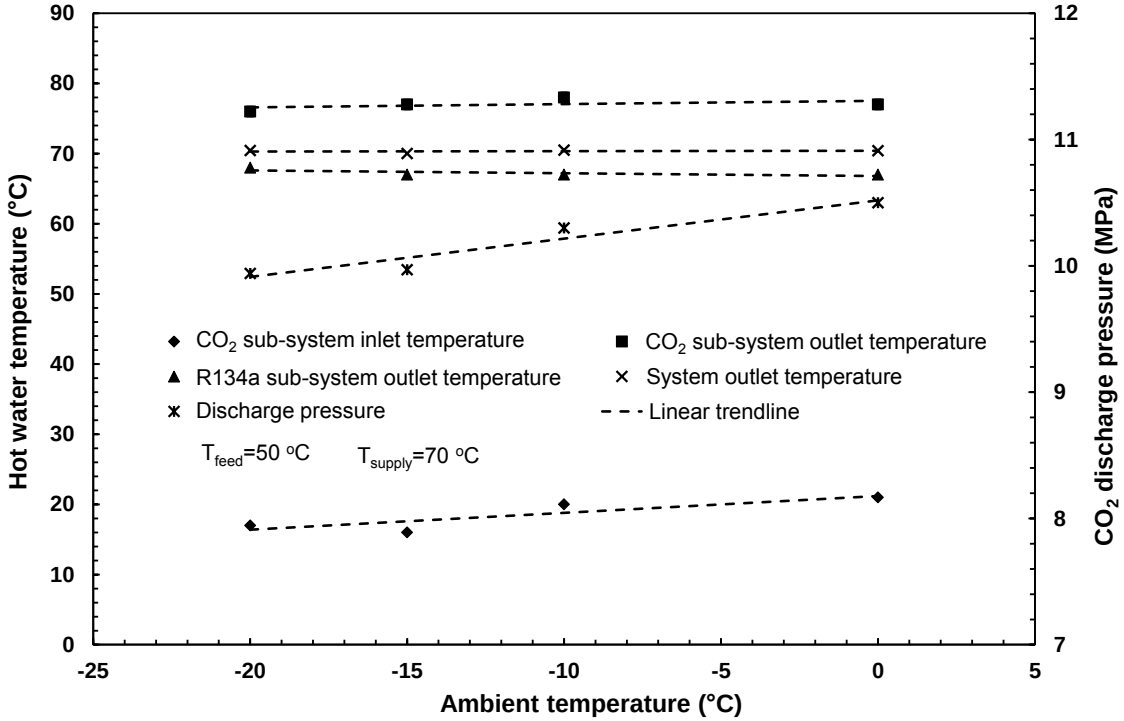

Fig. 6 Hot water temperature and CO_2 discharge pressure at the feed water temperature of 50 °C and water supply temperature of 70 °C.

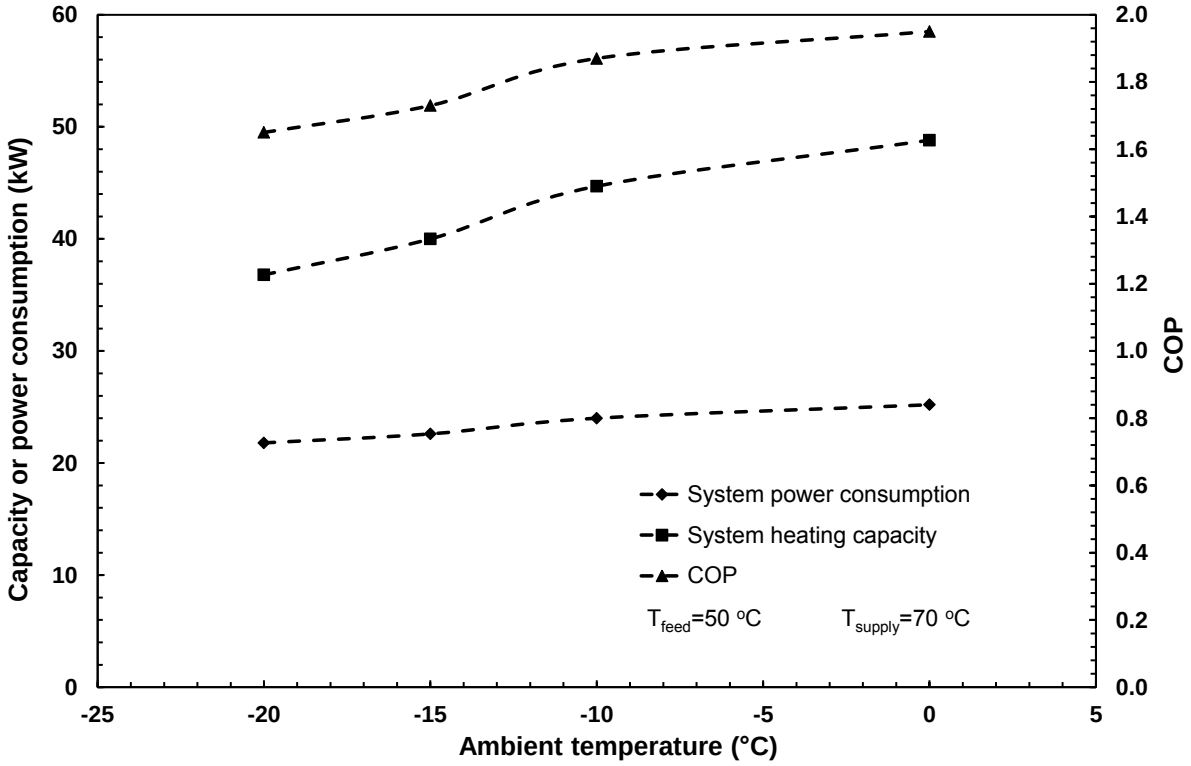

Fig. 7 System performance at the feed water temperature of 50 °C and water supply temperature of 70 °C.

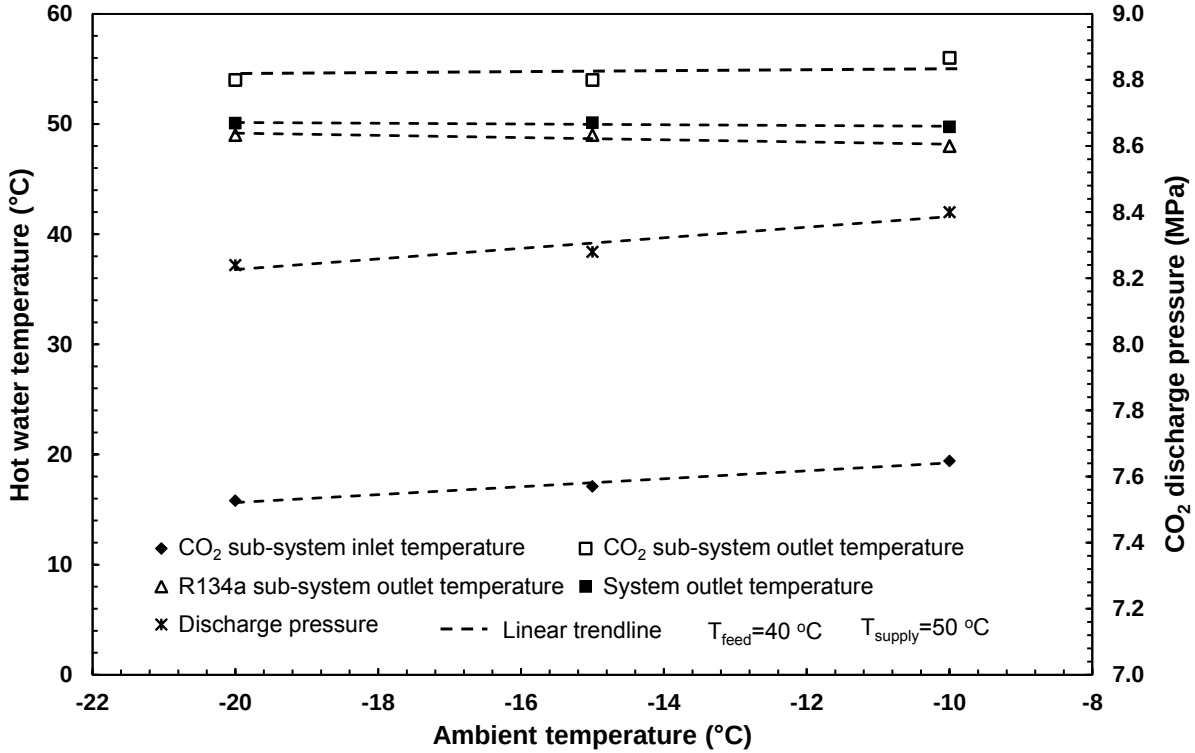

Fig. 8 Hot water temperature and CO_2 discharge pressure at the feed water temperature of 40 °C and water supply temperature of 50 °C.

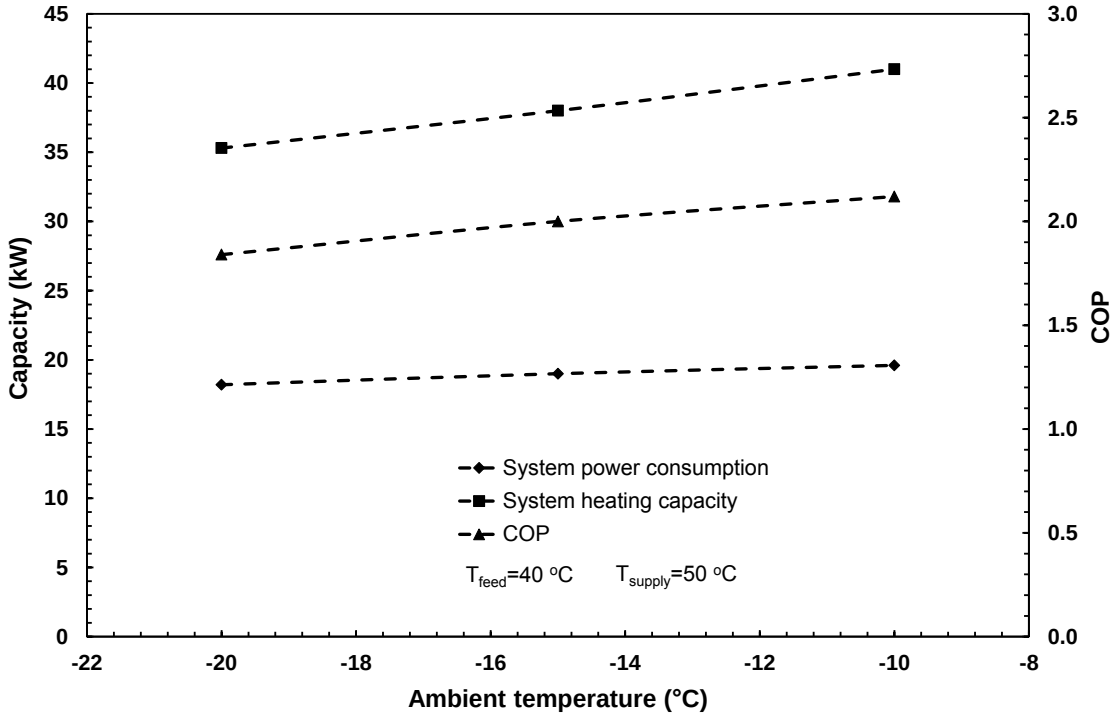

Fig. 9 System performance at the feed water temperature of 40 °C and water supply temperature of 50 °C.

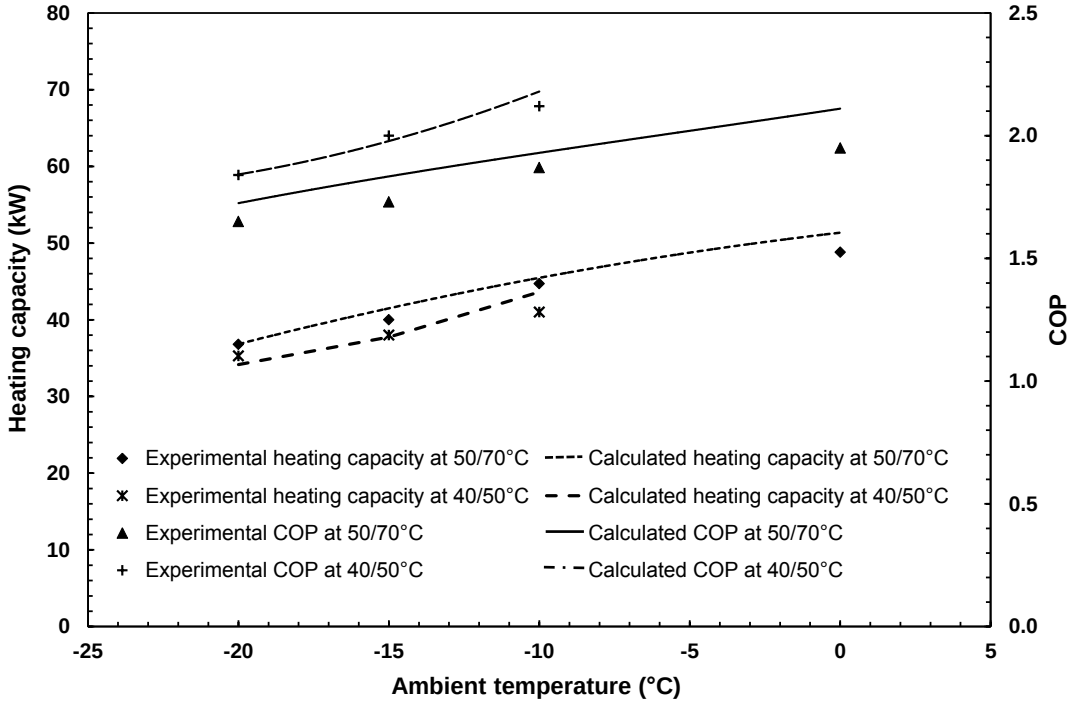

Fig. 10 Comparison between the simulated and experimental performance.

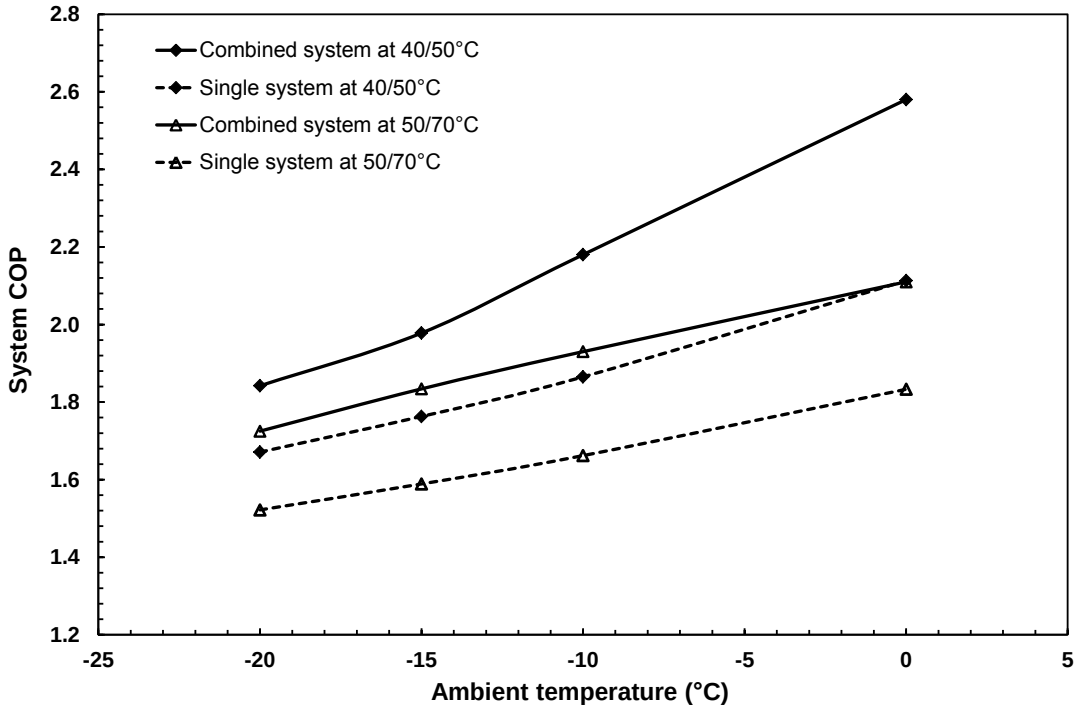

Fig. 11 Comparison between COPs of the standard transcritical CO_2 and combined systems

Table 1 Characteristics of the main components of the proposed system

Main components	Type	Characteristics
CO_2 compressor	(Bitzer) Semi-hermetic reciprocating compressor	Displacement: 12 $m^3 \cdot h^{-1}$
R134a compressor	(Copeland) Scroll compressor	Displacement: 35 $m^3 \cdot h^{-1}$
CO2 gas-ccoler	Tube in tube type	Outside tube: ϕ19× 2 mm stainless steel tube Inside tube: ϕ6.35 × 1 mm × 2 tubes Copper tube Length: 22 m × 4 groups in parallel
CO2 evaporator	V-Finned tube type	Tube diameter: 9.52 × 1 mm Tube length: 1.7 m Number of rows: 3 Number of tube per row: 40
R134a condenser	Tube in tube type	Outside tube: ϕ40 × 3 mm stainless steel tube Inside tube: ϕ9.52 × 0.36 mm × 9 Efficient finned copper tube Length 12.15m
R134a evaporator	Tube in tube	Outside tube: ϕ40 × 3 mm stainless steel tube Inside tube: ϕ9.52 × 0.36 mm × 9 Efficient finned copper tube Length 9.97m

Table 2 system COP at different flow ratio and space heating conditions

Water feed temperature of 50 °C and supply temperature of 70 °C (Total flow rate, 1430 $L \cdot hr^{-1}$)		Water feed temperature of 40 °C and supply temperature of 50 °C (Total flow rate, 1860 $L \cdot hr^{-1}$)	
Water flow ratio	COP	Water flow ratio	COP
78.9%	1.56	74.2%	1.86
77.6%	1.59	72.5%	1.88
76.0%	1.62	70.4%	1.85
73.4%	1.61	68.1%	1.84

*Water flow ratio is defined as the water flow rate to the R134a cycle condenser to the total water flow rate to the system.

Table 3 Assumptions and performance comparisons among different systems at ambient temperature of -10 °C, water feed temeprature of 50 °C and supply temeprature of 70 °C.

Comment [A2]: Author: There are two different Table 3 captions were provided, and this has been retained. Please check and confirm it is correct.

Items	Ejector system	Parallel compression system	Semi-cascade system without intermediate fluid	Proposed combined system
Power consumption (kW)	24.04	23.99	24.01	23.97
Heating capacity (kW)	32.3	35.3	46.6	46.3
COP	1.34	1.47	1.94	1.93
Heat transfer temperature difference between refrigerant and water/ refrigerant	5	5	5	5
Heat transfer temperature difference between refrigerant and air	10	10	10	10
Discharge pressure	11.5	11.8	10.38	10.3
Total superheating	5	5	5	5
Subcooling (if any)	_	_	3	3
Others	isentropic efficiency of nozzle=0.8 isentropic efficiency of diffuser=0.75	Economizer pressure=5.0MPa		